Published in final edited form as:
Lab Invest. 2013 November ; 93(11): 1254–1258. doi:10.1038/labinvest.2013.112.

Establishment of a system for monitoring endoplasmic reticulum redox state in mammalian cells

Kohsuke Kanekura[1,*], **Shinsuke Ishigaki**[2,*], **Philip I. Merksamer**[3], **Feroz R. Papa**[3,4,5,6], and **Fumihiko Urano**[1,§]

[1]Department of Medicine, Division of Endocrinology, Metabolism, and Lipid Research, Washington University School of Medicine, St. Louis, MO 63110, U.S.A

[2]Department of Neurology, Nagoya University Graduate School of Medicine, Nagoya 466-8550, Japan

[3]Department of Medicine, University of California San Francisco, CA 94143, U.S.A

[4]Diabetes Center, University of California San Francisco, CA 94143, U.S.A

[5]Lung Biology Center, University of California San Francisco, CA 94143, U.S.A

[6]California Institute for Quantitative Biosciences, University of California San Francisco, CA 94143, U.S.A

Abstract

The endoplasmic reticulum (ER) performs a critical role in the oxidative folding of nascent proteins such that perturbations to ER homeostasis may lead to protein misfolding and subsequent pathological processes. Among the mechanisms for maintaining ER homeostasis is a redox regulation, which is a critical determinant of the fate of ER stressed cells. Here we report the establishment of a system for monitoring ER redox state in mammalian cells. The new ER redox sensing system was developed based on the previously described monitoring system in yeast. Our system could successfully monitor the dynamic ER redox state in mammalian cells. Using this system, we find that manipulation of ER oxidases changes ER redox state. The mammalian ER redox sensing system could be used to study the mechanisms of ER redox regulation and provide a foundation for an approach to develop novel therapeutic modalities for human diseases related to dysregulated ER homeostasis including diabetes, neurodegeneration and Wolfram syndrome.

The ER participates in many important cellular tasks, including protein and lipid biosynthesis, calcium regulation, redox regulation, cell signaling, and cell death. Given the many vital and complex functions of the ER, it is little wonder that its failure can trigger a range of diseases including diabetes, neurodegeneration, and Wolfram syndrome, a genetic form of diabetes and neurodegeneration (1–6). The major mechanisms for maintenance of ER homeostasis include redox state regulation and activation of the unfolded protein

[§]Address correspondence to: Fumihiko Urano, M.D., Ph.D., Department of Medicine, Washington University School of Medicine, MO 63110, U.S.A., Phone: (314) 362-8683; Fax: (314) 362-8265, urano@dom.wustl.edu.
[*]These authors contributed equally to this work.

response (UPR), an adaptive response to the accumulation of misfolded proteins in the ER (1) (7).

The redox potential of the ER is continually preserved as an oxidizing environment to facilitate the oxidative process of disulfide bond formation during protein folding (7). In contrast, the UPR is an on-demand, adaptive regulatory response that controls diverse processes including protein folding, protein degradation, and ER biogenesis (1). In yeast cells, it has been shown that ER redox regulation and the UPR are tightly connected and disruption of ER redox state triggers the UPR and vice versa (8). However, in mammalian cells, the coordination of ER redox regulation and the UPR and their specific contributions to cell survival or death have yet to be elucidated due to the lack of a system for real-time monitoring of ER redox state. To address this critical gap in our understanding of the mechanisms for maintenance of ER homeostasis, we developed a system for real-time monitoring of ER redox state in mammalian cells.

Results

To visualize the ER redox state in mammalian cells, we adapted the previously described monitoring system in yeast for use in mammalian cells (8). To establish an ER-specific redox sensor, we appended the signal sequence of mouse BiP and the mammalian ER retrieval signal, KDEL, to the N-terminus and C-terminus of the redox-sensitive green fluorescent protein (GFP), respectively (Figure 1A) (8–10). This recombinant protein, termed MERO-GFP (Mammalian Endoplasmic reticulum-localized RedOx-sensitive GFP), localized to the ER following transient transfection (Figure 1B). MERO-GFP displayed distinct excitation spectra in the fully oxidized and reduced species, with maxima at 394 nm and 473 nm respectively (Figure 1C). The emission spectra from two distinct excitation wavelengths, 508 nm (Figure 1D) and 510 nm (Figure 1E), were comparable. Confocal microscopic analysis confirmed that fluorescence from the 476 nm excitation peak significantly increased while fluorescence from excitation 405 nm slightly decreased in cells treated with the strong reducing agent dithiothreitol (DTT). As a result, the ratio of the fluorescence from excitation 476 nm versus 405 nm significantly increased (Figure 1F). The fluorescence ratio between excitation 488 nm versus 405 nm normalized to wild-type untreated cells is called the MERO-GFP ratio. Treatment with H_2O_2, a strong oxidizing agent, did not change the MERO-GFP ratio, indicating that MERO-GFP is almost 100 % oxidized *in vivo*, consistent with the highly oxidizing environment of the ER (Figure 1G). In contrast, DTT treatment increased the MERO-GFP ratio in a dose-dependent manner, as expected (Figure 1G). Next, we monitored the MERO-GFP ratio in DTT treated cells at different time points. Within a few minutes of treatment with DTT, the ER was fully reduced and returned to an oxidized environment within a minute of DTT washout (Figure 1H). To confirm that the MERO-GFP ratio reflected changes in its redox state *in vivo*, we monitored the redox state of MERO-GFP using non-reducing SDS-PAGE in combination with the thiol-alkylating reagent, 4-acetamido-4′-maleimidylstilbene-2, 2′-disulfonic acid (AMS). As expected, non-reducing SDS-PAGE of lysates from untreated cells showed a rapidly migrating band of MERO-GFP while lysates from DTT-treated cells showed only one slowly migrating form of MERO-GFP. These results indicate that MERO-GFP is fully oxidized in the ER *in vivo* and becomes fully reduced following DTT treatment (Figure 1I).

These results propose that MERO-GFP can be used for real-time, live-monitoring of the redox state within the ER of mammalian cells.

To precisely monitor the MERO-GFP ratio *in vivo*, we used flow cytometry to measure the ratio of fluorescence from excitation at 488 nm versus 405 nm. DTT treatment increased the MERO-GFP ratio in the pancreatic β cell line, INS-1 832/13 cells, in a dose-dependent manner (Figure 2A and 2B). Although DTT treatment increased the MERO-GFP ratio, H_2O_2 treatment did not change the MERO-GFP ratio (Figure 2C and 2E), indicating that MERO-GFP was almost fully oxidized in the ER at basal levels. Compared with MERO-GFP, cytosolic roGFP (cyto-roGFP) was almost fully reduced at basal level, and was reduced and oxidized by treatments with DTT and H_2O_2 respectively (Figure 2D and 2E).

To assess if MERO-GFP monitors the dynamic ER redox state in mammalian cells, we manipulated the expression of key regulators of ER redox state and then monitored the ER redox state in mammalian cells stably expressing MERO-GFP. ER oxidoreductin-1α (ERO1α) is an ER-resident oxidase and one of the major regulators of ER redox state (7, 11). Suppression of ERO1α expression by shRNA directed against ERO1α increased the MERO-GFP ratio in HEK293a cells treated with DTT in a dose-dependent manner (Figure 3A, 3B, 3C and 3D). Suppression of another ER-resident oxidase, Peroxiredoxin IV (PRDX4) (12), by shRNA also increased the MERO-GFP ratio in HEK293a cells treated with DTT in a dose-dependent manner (Figure 3B, 3C and 3D). These results indicate that suppression of ER-resident oxidases impairs oxidizing capacity of the ER to maintain ER redox homeostasis. The difference between control cells and ERO1α-knockdown cells or PRDX4 knockdown cells was enhanced in the presence of DTT, suggesting that the oxidizing capacity of the ER can be precisely assessed when cells are challenged with a reducing agent such as DTT.

To further examine the ER redox regulation in different types of mammalian cells, we monitored the MERO-GFP ratio in HEK293a cells and INS-1 832/13 cells, a rodent β cell line, treated with different concentrations of DTT. The results shown in Figure 3E indicate that INS-1 832/13 cells are more susceptible to DTT-mediated reduction of the ER as compared to HEK293a cells. Collectively, these results indicate that MERO-GFP can monitor the dynamic ER redox state in different types of mammalian cells.

Discussion

Growing evidence indicates that dysregulation of ER homeostasis triggers a range of human chronic diseases, including diabetes, neurodegenerative diseases, and Wolfram syndrome (1–6, 13, 14). However, currently there is no effective therapy targeting the ER for such diseases due to the lack of a system which precisely monitors ER homeostasis. It has been established that the redox regulation is one of the major components for maintaining ER homeostasis. In this study, we report a new method for real-time monitoring of ER redox state in mammalian cells based on prior methods. Using this new method, we could confirm that ER oxidases play an important role in maintaining an oxidizing environment in the ER. We also revealed that different cell types might have different capacity of oxidative protein folding in the ER.

It has been proposed that chemical compounds that have the ability to manipulate the ER can be used for treating diseases associated with ER stress (15). We could utilize our method for identifying chemical compounds that can maintain an oxidizing environment in the ER under pathological conditions. We could also assess the roles of genes and proteins that can potentially manipulate ER redox state. Future studies will focus on use of this system in human samples to identify genes, proteins, and chemical compounds that can modify ER functions.

Materials and Methods

Reagents

Glucose, DTT, 4-acetamido-4′-maleimidylstilbene-2,2′-disulfonic acid (AMS), and cycloheximide were obtained from Sigma-Aldrich (St. Louis, MO). RPMI-1640 and DMEM were obtained from Invitrogen (Carlsbad, CA). Short hairpin RNA constructs (TRC) were obtained from RNAi core of University of Massachusetts Medical School. Anti-GFP antibody was purchased from Santa Cruz Biotechnology (Santa Cruz, CA).

Plasmid constructions

For constructing MERO-GFP plasmid, we appended the signal sequence of human BiP and the mammalian ER retrieval signal, KDEL, to the N-terminus and C-terminus of the redox-sensitive green fluorescent protein (GFP)-1, respectively.

Cell culture

INS-1 832/13 cells were cultured in the RPMI-1640 containing 10% fetal bovine serum (FBS), penicillin and streptomycin, sodium pyruvate and 0.1% β-mercaptoethanol. Human embryonic kidney 293A (HEK293A) and NSC34 cells were cultured in DMEM containing 10% FBS and penicillin and streptomycin. For establishing stable cell lines, cells were transduced with lentivirus expressing MERO-GFP and selected with puromycin or neomycin.

FACS analyses

For flow cytometry analyses, INS-1 832/13 and HEK293A expressing MERO-GFP were plated onto 12-well plates, treated with each compound for indicated times, and then harvested by trypsinization. After washing with PBS, cells were resuspended in the PBS. Flow cytometry analyses were performed with LSRII (BD) at the FACS core facility of University of Massachusetts Medical School and Washington University School of Medicine. The results were analyzed by FlowJo ver.7.6.3.

Short hairpin RNA (shRNA)

Control shRNA vector: pLKO.1-puro (Addgene, Cambridge, MA). shERO1L: TRCN0000059755, GCCAGAAAGTGGACCTAGTTA (Broad Institute, Cambridge, MA). shPRDX4: TRCN0000064821, GCTGTGATCGATGGAGAATTT (Broad Institute, Cambridge, MA)

Quantitative Real-Time PCR

Total RNA was extracted by RNeasy kits (Qiagen). Reverse transcriptiase PCR were performed using ImPromII (promega) reverse transcriptase and quantitative PCR was performed with Biorad iQ5 using SYBR green dye.

Plate reader

The excitation spectra and emission spectra of MERO-GFP were determined by SAFIRE (Tecan). INS-1 832/13 cells were plated onto a 96 well plate at 50,000 cells/well and the emission spectra and excitation spectra were scanned by SAFIRE in 1nm increments. Working range of MERO-GFP was also determined by SAFIRE. INS-1 832/13 cells were plated onto 96 well plates, treated with H_2O_2 or DTT at various concentrations for 30 min and then the fluorescence at excitation wavelength 473 nm and emission wavelength 510 nm (for reduced MERO-GFP) or at excitation wavelength 394 nm and emission wavelength 510 nm (for oxidized MERO-GFP) was measured. After subtraction of background signal, the MERO-GFP ratio was determined.

AMS-modified SDS-PAGE

INS-1 832/13 cells untreated or treated with 2 mM DTT were lysed with 1x SDS-PAGE sample buffer containing 25 mM AMS with or without -mercaptoethanol, boiled at 95°C for 10min, and applied to SDS-PAGE followed by immunoblotting with anti-GFP antibody.

Statistical analyses

Percent of positive cells (y) was measured as a proportion of positive cells among all GFP-positive cells treated. Frequently arcsine [sqrt (y)] transformation is applied to the raw data to homogenize the variance before further data analysis (16). Therefore, all the analysis for percent of positive cells was performed on transformed data. A set of predetermined contrasts were performed in the framework of one-way ANOVA in R.

Acknowledgments

We thank Karen Sargent, Cris Brown, and Mai Kanekura for technical assistance and Agata Jurczyk, Richard Konz and Takeshi Egawa for technical advice. This work was supported by grants from NIH (DK067493, DK016746, P60 DK020579, and UL1 TR000448), JDRF (47-2012-760), ADA (1-12-CT-61), and the Jack and J.T. Snow Scientific Research Foundation to F. Urano and the Grant-in-Aid for Exploratory Research/JST to S. Ishigaki. K. Kanekura was partly supported by fellowships from the Japan Society for the Promotion of Science and Uehara Memorial Foundation.

References

1. Walter P, Ron D. The unfolded protein response: from stress pathway to homeostatic regulation. Science. 2011; 334(6059):1081–1086. [PubMed: 22116877]
2. Scheuner D, Kaufman RJ. The unfolded protein response: a pathway that links insulin demand with beta-cell failure and diabetes. Endocr Rev. 2008; 29(3):317–333. [PubMed: 18436705]
3. Oslowski CM, Urano F. The binary switch that controls the life and death decisions of ER stressed beta cells. Curr Opin Cell Biol. 2011; 23(2):207–215. [PubMed: 21168319]
4. Hotamisligil GS. Endoplasmic reticulum stress and atherosclerosis. Nature medicine. 2010; 16(4): 396–399.

5. Hotamisligil GS. Endoplasmic reticulum stress and the inflammatory basis of metabolic disease. Cell. 2010; 140(6):900–917. [PubMed: 20303879]

6. Ozcan L, Tabas I. Role of endoplasmic reticulum stress in metabolic disease and other disorders. Annual review of medicine. 2012; 63:317–328.

7. Tu BP, Weissman JS. Oxidative protein folding in eukaryotes: mechanisms and consequences. The Journal of cell biology. 2004; 164(3):341–346. [PubMed: 14757749]

8. Merksamer PI, Trusina A, Papa FR. Real-time redox measurements during endoplasmic reticulum stress reveal interlinked protein folding functions. Cell. 2008; 135(5):933–947. [PubMed: 19026441]

9. Dooley CT, et al. Imaging dynamic redox changes in mammalian cells with green fluorescent protein indicators. The Journal of biological chemistry. 2004; 279(21):22284–22293. [PubMed: 14985369]

10. Hanson GT, et al. Investigating mitochondrial redox potential with redox-sensitive green fluorescent protein indicators. The Journal of biological chemistry. 2004; 279(13):13044–13053. [PubMed: 14722062]

11. Cabibbo A, et al. ERO1-L, a human protein that favors disulfide bond formation in the endoplasmic reticulum. The Journal of biological chemistry. 2000; 275(7):4827–4833. [PubMed: 10671517]

12. Zito E, et al. Oxidative protein folding by an endoplasmic reticulum-localized peroxiredoxin. Molecular cell. 2010; 40(5):787–797. [PubMed: 21145486]

13. Fonseca SG, et al. WFS1 Is a Novel Component of the Unfolded Protein Response and Maintains Homeostasis of the Endoplasmic Reticulum in Pancreatic {beta}-Cells. The Journal of biological chemistry. 2005; 280(47):39609–39615. [PubMed: 16195229]

14. Fonseca SG, et al. Wolfram syndrome 1 gene negatively regulates ER stress signaling in rodent and human cells. The Journal of clinical investigation. 2010

15. Ozcan U, et al. Chemical chaperones reduce ER stress and restore glucose homeostasis in a mouse model of type 2 diabetes. Science. 2006; 313(5790):1137–1140. [PubMed: 16931765]

16. Freeman MF, Tukey JW. Transformations related to the angular, and the square root. Ann Mathem Stat. 1950; 21:607–611.

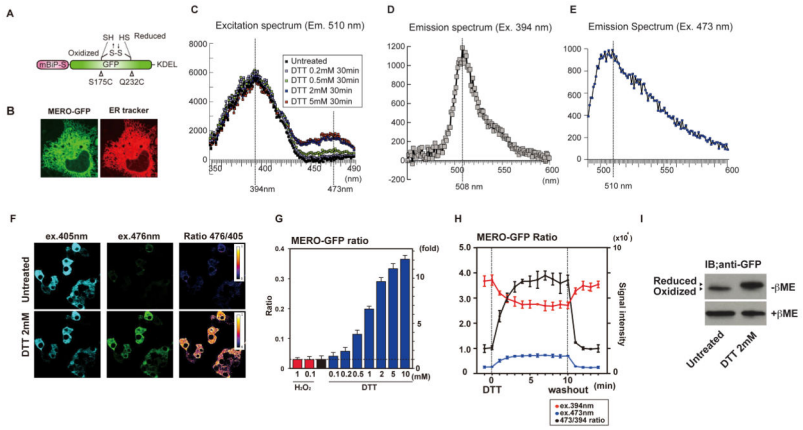

Figure 1. Characterization of MERO-GFP

(A) Schematic structure of MERO-GFP. (B) Confocal imaging of MERO-GFP in COS7 cells. ER was visualized by DsRed-ER tracker. (C) Excitation spectra of MERO-GFP treated with different concentrations of DTT. (D) Emission spectrum of oxidized MERO-GFP in untreated NSC34 cells. The wavelength of excitation was 394 nm. (E) Emission spectrum of reduced MERO-GFP in NSC34 cells treated with 2 mM DTT. The wavelength for excitation was 473 nm. (F) Real-time imaging of MERO-GFP signal from 476 nm excitation and 405 nm excitation in INS-1 832/13 cells treated with or without 2 mM DTT. 476/405 ratio images are displayed in false colors in the lookup table. (G) MERO-GFP ratio in cells treated with the indicated concentrations of DTT and H_2O_2. MERO-GFP ratio was determined by a plate reader. Data represents means ± SD from three independent experiments. (H) Real-time monitoring of MERO-GFP ratio in live NSC34 cells treated with DTT. NSC34 cells expressing MERO-GFP were treated with DTT (1 mM) and the fluorescence from MERO-GFP was measured every minute. Ten minutes after the treatment, DTT was washed out. The red line indicates the fluorescence intensity with excitation at 394nm. The blue line indicates the fluorescence intensity with excitation at 473 nm. Black line indicates the normalized MERO-GFP ratio. (I) AMS-modified SDS-PAGE of MERO-GFP. All error bars shown, ± s.d.

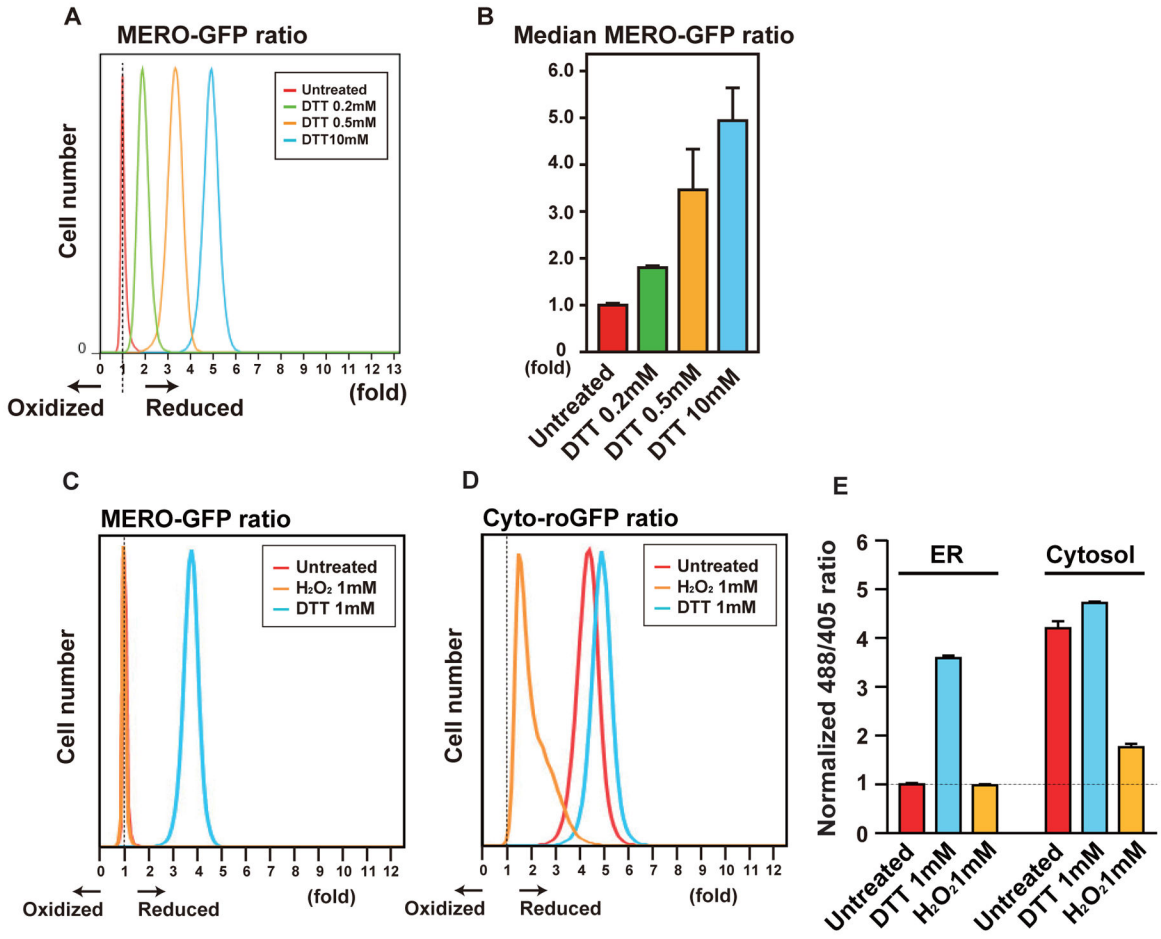

Figure 2. MERO-GFP is fully oxidized under normal conditions and reduced by DTT *in vivo*

(A) Histogram of INS-1 832/13 cells stably expressing MERO-GFP treated with DTT. The x-axis indicates the MERO-GFP ratio and the y-axis indicates the number of cells. All error bars shown, ± s.d. (B) The median MERO-GFP ratio of the data shown in Figure 2A. (C) Histogram of MERO-GFP ratio of untreated cells or cells treated with 1 mM H_2O_2 or 1 mM DTT. (D) Histogram of cytosolic roGFP (cyto-roGFP) ratio of untreated cells or cells treated with 1 mM H_2O_2 or 1 mM DTT. (E) The median of MERO-GFP or cytosolic roGFP ratio of untreated cells or cells treated with 1mM H_2O_2 or 1 mM DTT.

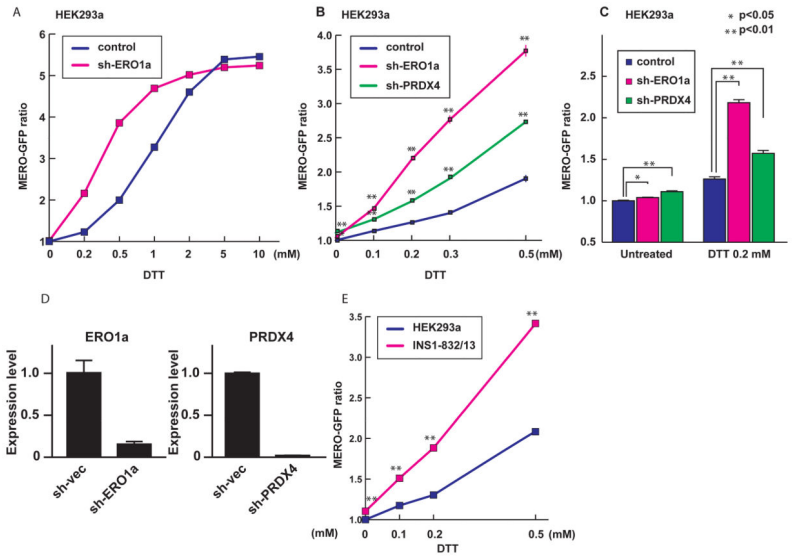

Fig. 3. MERO-GFP monitors the dynamic ER redox state in mammalian cells

(A) The MERO-GFP ratio in HEK293a cells transduced with control shRNA or shRNA directed against ERO1α and then treated with different concentrations of DTT. (B) The MERO-GFP ratio in HEK293a cells transduced with control shRNA, shRNA directed against ERO1α, or shRNA directed against PRDX4, and then treated with different concentrations of DTT. (C) The MERO-GFP ratio of HEK293a cells transduced with control shRNA, shRNA directed against ERO1α or shRNA directed against PRDX4, and treated with or without 0.2 mM DTT. (D) Expression levels of ERO1α and PRDX4 mRNA in HEK293a cells transduced with control shRNA or shRNA directed against ERO1α (left panel) or PRDX4 (right panel). Expression levels of mRNA were measured by real-time PCR. (E) The oxidizing capacity of the ER in different cell lines. All error bars shown, ± s.d. * $p<0.05$, ** $p<0.01$.